



## Green Synthesis of ZnO Nanoparticles Using Sweet Orange Peels as a Mediating Agent and their Antibacterial Properties

SUMITHRANAND V. B.<sup>1</sup>, ROXY M. S.<sup>2\*</sup> and VAISHNAVI G.<sup>2</sup>

<sup>1</sup>Department of Physics, Government College, Kariavattom, Thiruvananthapuram, Research Centre, University of Kerala, Kerala, India.

<sup>2</sup>Department of Physics, Sree Narayana College, Kollam, Research Centre, University of Kerala, Kerala, India.

\*Corresponding author E-mail: roxymys@gmail.com

<http://dx.doi.org/10.13005/ojc/400221>

(Received: January 20, 2024; Accepted: March 05, 2024)

### ABSTRACT

This study presents the environmentally friendly synthesis of *Citrus sinensis* bio-mediated Zinc Oxide (ZnO) nanoparticles. The characterization techniques, including XRD, UV-Visible spectroscopy, and FTIR, provide insight into the structural and optical properties of the synthesized nanoparticles. The determined average crystalline size using the Debye Scherrer equation is 15.57 nm, highlighting the nanoscale nature of the particles. The band gap energy of the sample was measured as 3.26 eV through UV-Visible spectroscopy. Furthermore, the antibacterial efficacy of the synthesized ZnO nanoparticles was assessed against *Salmonella typhimurium*, *Staphylococcus aureus*, *S. faecalis* and *E. coli*, using modified Kirby-Bauer disc diffusion method. The findings suggest the potential of these nanoparticles as effective antibacterial agents.

**Keywords:** Green synthesis, ZnO nanoparticles, Antibacterial studies, *Citrus sinensis*.

### INTRODUCTION

Nanomaterials have emerged as a pivotal cornerstone in contemporary research and technology, signifying a transformative era in various scientific disciplines. Their significance lies in their unique properties and the boundless potential they hold for innovation. At the nanoscale, these materials exhibit exceptional electrical, mechanical, and optical characteristics that deviate from their bulk counterparts, unlocking an abundance of applications. From advanced materials with improved strength and conductivity to nanoscale

drug delivery systems revolutionizing healthcare, nanomaterials continue to refine the boundaries of possibility. In the fields of electronics, energy, environmental science, and medicine, the influence of nanomaterials is profound, offering solutions to some of our most pressing challenges. As the bridge between the macroscopic and molecular worlds, nanomaterials epitomize the essence of interdisciplinary research, holding the promise of a sustainable and technologically advanced future.

Metal nanoparticles have significant interest, due to the size dependent physical



and chemical properties, as well as their high technological potential<sup>1</sup>. Zinc oxide nanoparticles (ZnO NPs) have emerged as prominent and versatile materials within the domain of metal oxides, garnering considerable attention across an array of scientific and industrial disciplines. Their extensive range of applications spans from enhancing industrial products<sup>2,3</sup> to revolutionizing the capabilities of sensors<sup>4,5</sup>, optoelectronic devices<sup>6</sup>, biomedicine<sup>7,8</sup>, and bioimaging<sup>9,10</sup>. Notably, ZnO NPs have also demonstrated their mettle in critical areas such as biomolecular detection diagnostics and microelectronics<sup>11</sup>. The traditional synthesis methods of ZnO NPs primarily involve chemical procedures that, while effective, come with their own set of challenges. These approaches often necessitate the use of expensive reagents and inadvertently generate toxic by-products, raising substantial environmental concerns<sup>12</sup>. In stark contrast, the advent of green-mediated synthesis has ushered in a more sustainable, eco-friendly paradigm. In chemical reduction methods, the reducing agent is a chemical solution, while in biological methods, a collection of enzymes, particularly reductases, acts as the reducing agent<sup>13</sup>. In this innovative approach, various components of plants, encompassing leaves, stems, vegetation, seeds, and roots, have proven to be invaluable bioresources for nanoparticle synthesis<sup>14-18,19</sup>. It is noteworthy that the utilization of fruit peels in nanoparticle synthesis represents an underexplored frontier, having piqued the curiosity of only a select group of pioneering researchers.

In the pursuit of an eco-conscious and biologically safe nanoparticle synthesis process, our

study embarks on a journey leveraging the versatile sweet orange peel as the fundamental agent. In doing so, we offer a cost-effective solution that contributes to the responsible and efficient synthesis of ZnO nanoparticles, opening new avenues of exploration in the nanomaterial's domain.

## EXPERIMENTAL

### MATERIALS AND METHODS

The synthesis of zinc oxide nanoparticles via a green-mediated approach is detailed in this procedure. Sweet oranges, scientifically known as *Citrus sinensis*, serve as the fundamental source for preparing these nanoparticles. The process commences with the extraction of sweet orange peels, which are meticulously dried and ground into a fine powder. This powdered material is then mixed with de-ionized water to achieve a 4% concentration, with continuous agitation for a duration of 3 hours. Subsequently, the mixtures are subjected to a water bath set at 90°C for an hour, after which they are filtered and securely stored in an inert atmosphere within glass containers.

In parallel, a solution consisting of 0.1M Zinc acetate [ $(\text{CH}_3\text{COO})_2 \text{Zn} \cdot 2\text{H}_2\text{O}$ ] is prepared, with a total volume of 400 mL. This solution is heated to a temperature of 65°C. At this stage, 40 mL of the previously prepared citrus sinensis peel extract is introduced into the conical flask, while maintaining the specified temperature. A remarkable transformation occurs, as the colorless zinc acetate solution instantaneously turns from its original state to a pale-yellow hue.

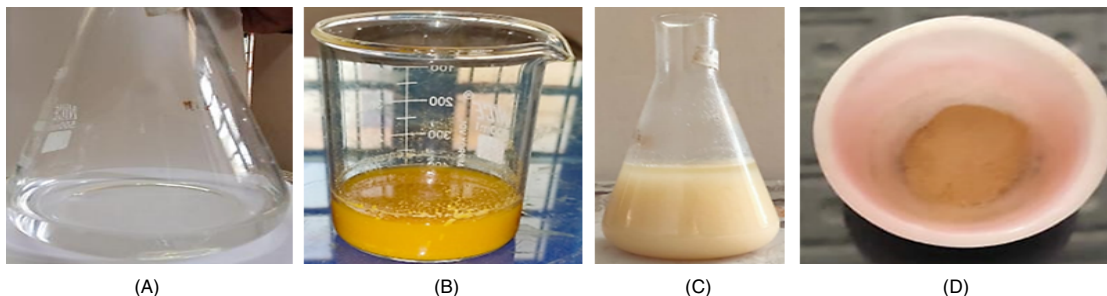


**Fig. 1. Preparation of nanoparticles (A) Zinc Acetate solution (B) Orange peel extract (C) Mixture of Orange peel extract and Zinc Acetate solution (D) Synthesized ZnO nanoparticles**

For a comprehensive and precise synthesis, the mixture is stirred vigorously for a duration of 4 hours. This stirring causes the formation of ZnO

nanoparticles, substantiated by a vivid colour shift from pale yellow to a distinctive cream-white. At this juncture, the mixture is permitted to cool up to room

temperature. It is then subjected to centrifugation at 5000 rpm, for 25 minutes. The obtained precipitate is thoroughly washed twice with deionized water to ensure the removal of any residual impurities. The white precipitate, now a promising assembly of zinc oxide nanoparticles, is meticulously oven-dried and carefully stored, used for further comprehensive characterization. This method represents an eco-conscious and biologically safe approach, utilizing readily available citrus resources to synthesize valuable nanomaterials.

### Characterization methods

The characterization and evaluation of the synthesized ZnO nanoparticles involved a comprehensive array of techniques and tests. X-ray powder diffraction patterns were acquired using an XRD instrument, utilizing Cu-K $\alpha$ 1 with  $\lambda=1.5406$  Å. The diffraction data were meticulously recorded in the range (2 $\theta$ ) spanning from 20° to 80°. This analysis served to provide critical insights into the structural properties of the nanoparticles. Fourier-Transform Infrared (FTIR) spectra of the ZnO nanoparticles were meticulously recorded across a spanning range of 4000 cm<sup>-1</sup> to 400 cm<sup>-1</sup>. This provided valuable information on the chemical bonds and functional groups present within the synthesized nanoparticles. The UV-Visible absorption spectra was used to analyze the optical properties of the nanoparticles. The spectrum was scaled over a wavelength range of 200 to 700 nm, offering a detailed exploration of the nanoparticles' behavior under different wavelengths of light.

To assess the antibacterial activity of the prepared samples, Kirby-Bauer disc method in modified form was employed. The relevant microorganisms, with pure cultures were propagated in Miller Hinton broth under controlled conditions. A bacterial lawn was meticulously prepared by evenly spreading a fresh culture, with a concentration of 10<sup>6</sup> colony forming units per mL on nutrient agar plates for each of the test organism. The antimicrobial activity of the synthesized nanomaterial was assessed by carefully punching the wells of 8 mm in diameter into the agar plates, following a brief absorption period. In order to prevent the unintended leakage of the nanomaterial, so as to ensure the precision, molten agar (0.8% agar) was used to seal the wells. subsequently, 100 micro liters (equivalent to 50 micrograms) of the nanoparticle

suspension were introduced on each well of every plates. It was kept at 35°C $\pm$ 2°C, for an overnight period of incubation. The extension in inhibition zone around the disc was meticulously measured in millimeters, quantifying the antimicrobial effect of the ZnO nanoparticles. In this context, a blank of solvent was act as the negative control. At the same time antibiotic tetracycline served for the positive control, facilitating a comprehensive assessment of the synthesized nanoparticles' antibacterial efficacy.

## RESULTS AND DISCUSSION

### XRD Characterization studies

The XRD pattern of the synthesized ZnO nanoparticles is a crucial element, as it offers insights into the crystalline structure and purity of the nanoparticles. As illustrated in Fig. 2, the XRD spectra of the synthesized ZnO nanoparticle sample unveil intriguing characteristics. Within the XRD pattern, one can observe peak broadening, a phenomenon that is indicative of the presence of nanocrystals with relatively small dimensions in the sample. This broadening of the peaks is a characteristic feature of nanomaterials and underscores the nanoscale nature of the ZnO particles under investigation. Moreover, the XRD pattern reveals the presents of strong diffraction peaks, which is an affirming indicator of the crystalline nature of the synthesized ZnO nanoparticles. These diffraction peaks conform to the well-documented wurtzite pattern, signifying the specific crystalline structure adopted by the ZnO nanoparticles. The wurtzite pattern is the standard crystal structure associated with ZnO, and its presence reinforces the high degree of crystallinity and structural purity in the synthesized nanoparticles.

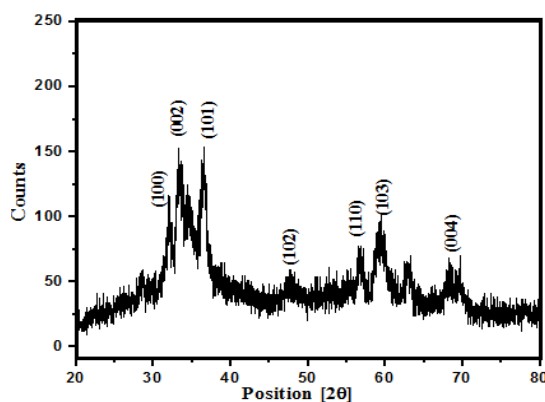


Fig. 2. XRD pattern of ZnO nanoparticles synthesised using orange peel extract

The X-ray diffraction (XRD) analysis has yielded detailed information about the crystalline structure of the synthesized ZnO nanoparticles. The diffraction peaks observed in the XRD spectra are attributed to specific crystallographic planes, providing insight into the precise orientation and arrangement of the nanoparticles<sup>20</sup>. In particular, the XRD analysis has identified the following crystallographic planes for different peaks; (100) (002) (101) (102) (110) (103) and (004). These peaks are positioned at specific  $2\theta$  values are  $31.68^\circ$ ,  $33.51^\circ$ ,  $36.52^\circ$ ,  $47.7^\circ$ ,  $56.63^\circ$ ,  $62.83^\circ$ , and  $86.91^\circ$ , respectively. Remarkably, these observed peak positions align perfectly with the standard pattern for ZnO, as defined by the Joint Committee on Powder Diffraction Standards (JCPDS). The ZnO crystal structure, indexed as the hexagonal wurtzite structure, is in complete accordance with the measured peak positions. Notably, the (101) plane, with a  $2\theta$  value of  $36.52^\circ$ , exhibits the maximum intensity, indicating its prominence in the synthesized ZnO nanoparticles.

It's worth mentioning that the presence of certain undesirable peaks can be attributed to the formation of side products during the synthesis process. This phenomenon is expected, as plant extracts contain a myriad of compounds, and these impurities can result in the emergence of additional diffraction peaks. Nonetheless, the dominant presence of the desired ZnO diffraction peaks signifies the successful formation of ZnO nanoparticles having hexagonal wurtzite in structure, a crucial finding in the characterization of these nanomaterials.

The analysis of the crystalline structure of the ZnO nanoparticles involves the application of Bragg's law, a fundamental principle in X-ray diffraction. Bragg's law is expressed as :

$$2d\sin\theta = n\lambda \quad (1)$$

In this equation, "d" represents the interplanar distance between two diffraction planes, " $\theta$ " is the scattering angle, "n" – the order of diffraction, " $\lambda$ " – the wavelength of incident X ray. For a hexagonal crystal with lattice parameters "a" and "b", the interplanar distance for the planes defined by Miller indices (hkl) and allow the calculation of "a" and "c" in ZnO hexagonal structure. Furthermore,

the interplanar spacing " $d_{hkl}$ " for different orientations of the sample can be calculated<sup>21</sup>. The calculated values can then be compared with the JCPDS standard "d" values to confirm the formation of ZnO. The calculation of particle size is one of the most important characteristics of nanoparticles<sup>22</sup>. The average crystalline size of the ZnO nanoparticles is calculated by the Debye-Scherrer formula, expressed as<sup>23</sup>.

$$D = \frac{0.9\lambda}{\beta\cos\theta} \quad (2)$$

Here, " $\lambda$ " – the wavelength of incident X ray, " $\beta$ " – full width at half maximum (FWHM) in radians, and " $\theta$ " – the scattering angle in degrees. Using this formula, the average crystalline size is obtained as 15.57 nm. Additionally, the volume of the hexagonal primitive cell is determined using the equation<sup>24</sup>.

$$V_c = \frac{\sqrt{3}}{2} a^2 c \quad (3)$$

Where " $V_c$ " denotes the volume of the crystal primitive cell. The calculated value of  $V_c$  is  $49.16 \text{ \AA}^3$ , providing further insights into the structural characteristics of the ZnO nanoparticles.

### UV-Visible studies

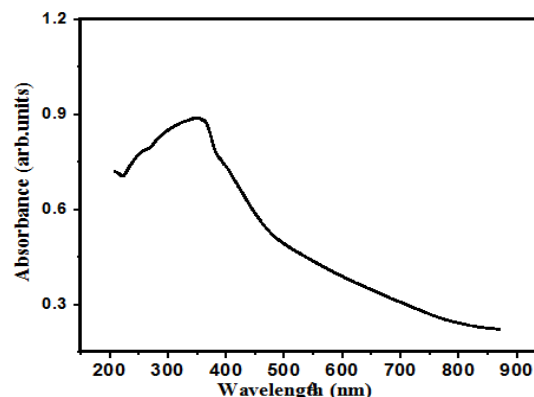


Fig. 3. Absorption spectrum of ZnO nanoparticles

The UV-Visible spectrum, as depicted in Fig. 3, serves as a critical piece of evidence confirming the reduction of pure  $Zn^{2+}$  ions and providing valuable insights into the optical properties of the ZnO nanoparticles. In particular, the determination of the optical band gap is a significant aspect of this analysis. Within the material, an electron required the minimum energy for its transition from valence band to conduction band, which is termed as optical band gap. This transition is fundamentally linked to the absorption of photons.

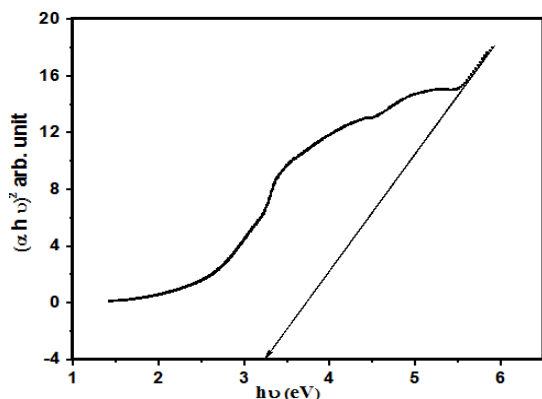


Fig. 4. Determination of band gap of ZnO nanoparticles

Using the following equation, the direct absorption band gap can be calculated from the obtained absorption data<sup>25</sup>

$$\alpha h\nu = B(h\nu - E_g)^n \quad (7)$$

In this equation, " $\alpha$ " – absorption coefficient, " $B$ " – material specific constant, " $h\nu$ " – photon energy, " $E_g$ " – optical band gap of the material, and " $n$ " – parameter used to distinguish between direct and indirect transitions. When " $n$ " is equal to 2, it signifies a direct transition, while " $n$ " as  $\frac{1}{2}$  indicates an indirect transition. The application of this equation to the absorption data from the UV-Visible spectrum enables the determination of the direct band gap of the ZnO nanoparticles, which is obtained as 3.26 eV, providing crucial information about their optical properties and behavior in response to photon excitation.

### FTIR studies

The Fourier-Transform Infrared (FTIR) spectroscopy analysis played a pivotal role in examining the various phytochemicals, which causes bio reduction of the metal precursor, to the respective metal oxide nanoparticles. The FTIR spectrum of the ZnO nanoparticles recorded within the range of 4000-400  $\text{cm}^{-1}$ , is depicted in Figure 5.

Within this spectrum, several distinct peaks and bands have been identified, shedding light on the chemical composition and functional groups present in the synthesized ZnO nanoparticles. Notably, the peaks observed within the range of 400 to 700  $\text{cm}^{-1}$  can be primarily attributed to the stretching modes of ZnO, revealing the characteristic vibrations associated with this material<sup>26</sup>. Furthermore, the spectrum exhibits a prominent peak at 3300  $\text{cm}^{-1}$ , corresponding to a strong broadband associated with the presence of -OH groups. The attached -OH

groups to the nanoparticle surface, are commonly exists in organic molecules, highlighting their role in the bio reduction process. Additional peaks at specific wavenumbers gives information about the composition of nanoparticles. For instance, peaks at 1557  $\text{cm}^{-1}$ , 1378  $\text{cm}^{-1}$ , 1018  $\text{cm}^{-1}$ , and 928  $\text{cm}^{-1}$  are associated with various chemical vibrations. These vibrations are associated with carbonyl stretch, in plane C-OH bending, carboxylic acid vibrations, and C-O bending, as well as out of plane -CH bending vibrations in trans or E alkenes respectively<sup>27,28</sup>. These specific peaks and bands in the FTIR spectrum offer essential clues regarding the organic molecules and functional groups involved in the bio reduction process, contributing to a comprehensive understanding of the synthesis of ZnO nanoparticles.

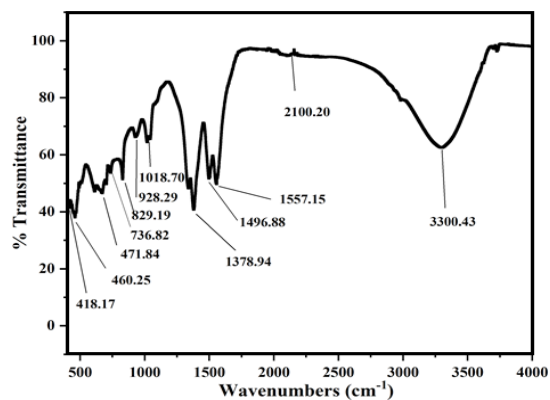


Fig. 5. FTIR spectrum of ZnO nanoparticles

### Antibacterial activity of ZnO nanoparticles

Modified Kirby Bauer disc method was used to assess the antibacterial activity of the prepared ZnO nanoparticles, as illustrated in Fig. 6. The obtained results of this evaluation are summarized in Table 1, and provide valuable insights into the nanoparticles' effectiveness against specific bacterial strains.

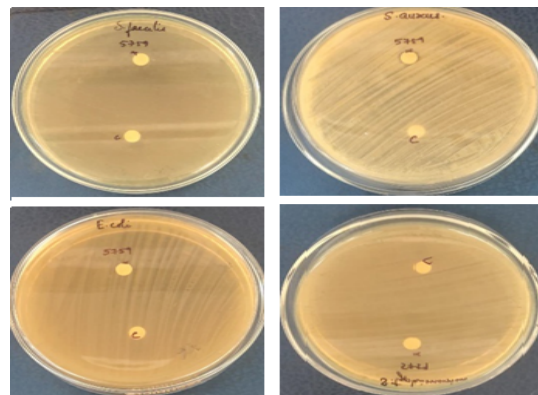


Fig. 6. The viability of *S. faecalis*, *S. aureus*, *E. coli*, and *S. typhimurium* with ZnO nanoparticles

The results indicates that the ZnO nanoparticles exhibited significant antibacterial properties. Specifically, at a concentration of 10 mg/mL, the nanoparticles generated an antibacterial inhibition zone of 7 mm when tested against *Salmonella typhimurium* and *Streptococcus faecalis*. Moreover, the nanoparticles displayed a slightly larger inhibition zone of 9 mm when challenged by *Staphylococcus aureus* and *Escherichia coli*. These findings underscore the potential of the ZnO nanoparticles as effective antibacterial agents. The results indicate their capacity to prevent the growth and proliferation of these bacterial strains, highlighting their promising role in combating microbial infections. Such antibacterial properties make these nanoparticles valuable for various biomedical and healthcare applications, where the control of bacterial pathogens is of paramount importance. Studies reported that silver nanoparticles coated paper can be successfully used for inhibiting or reducing *Gram-negative E. coli* and *Gram-positive S. aureus* bacteria<sup>29</sup>.

**Table 1: Comparison of antibacterial activity of ZnO nanoparticles**

Bacteria	Results (mm)
<i>S. typhimurium</i>	7
<i>S. aureus</i>	9
<i>S. faecalis</i>	7
<i>E. coli</i>	9

The relationship between nanoparticle size and their antimicrobial efficacy is indeed a critical factor in understanding their action against microorganisms. The antimicrobial activity of nanoparticles is significantly influenced by the surface area available for interaction with microorganisms. When nanoparticles are reduced in size, their surface area-to-volume ratio increase substantially. This heightened surface area enhances the chemical reaction by increasing the number of active sites. In the context of antimicrobial action, it means that more nanoparticles can come into contact with microorganisms, leading to enhanced microbial interactions. This phenomenon is often attributed to several factors. Firstly, the increased surface area provides more binding sites for nanoparticles to attach to microbial cell surfaces. These interactions can disrupt cell membranes, interfere with cellular processes, and ultimately lead to the inhibition or destruction of microorganisms. Additionally, the increased surface area allows for

greater exposure of functional groups or chemical properties on the nanoparticle surface, which can further enhance their antimicrobial properties<sup>30</sup>. In summary, the size-dependent increase in surface area is a crucial aspect of nanoparticle microbial activity, as it promotes more efficient interactions with microorganisms and, consequently, more effective inhibition or eradication of microbial populations. This understanding is fundamental in the design and application of nanoparticles for various antimicrobial and biomedical purposes.

## CONCLUSION

This study focuses on bio synthesis of ZnO nanoparticles, which were produced through an environmentally friendly approach involving the use of orange peel extracts. The nanoparticles were subjected to a thorough characterization process to understand their properties and potential applications. The characterization techniques included XRD, UV-Visible spectroscopy, and FTIR. The XRD analysis confirmed the formation of pure wurtzite-structured ZnO nanoparticles, a critical finding in determining their crystalline structure. The XRD data also allowed for the calculation of particle size and lattice parameters, with an average crystalline size of approximately 15.57 nm. UV-Visible spectroscopy provided the optical properties of the ZnO nanoparticles, which revealed a direct band gap of 3.26 eV. The obtained band gap measurement is consistent with values previously reported for ZnO nanoparticles, indicating the high quality and purity of the synthesized material. The FTIR spectroscopy analysis provided insights into the chemical bonds present in the nanoparticles, shedding light on the nature of the synthesized samples and the organic molecules involved in their formation. The nanoparticles were tested against several pathogenic bacterial strains, including, *S. faecalis*, *S. aureus*, *E. coli*, and *S. typhimurium*. The inhibition zones present in the antibacterial tests clearly demonstrated the nanoparticles' effectiveness in inhibiting the growth of these bacteria. In summary, the study concludes that the environmentally friendly, green-synthesized ZnO nanoparticles exhibit strong antibacterial properties against a range of pathogenic bacteria. This research holds promise for potential applications of these nanoparticles, in various biomedical and healthcare-related fields where the control of the bacterial infection is crucial.

**ACKNOWLEDGEMENT**

The authors are grateful to the anonymous reviewers for their valuable comments and suggestions.

**Conflicts of Interest**

The authors declare that there is no conflict of interest regarding the publication of this paper.

**REFERENCES**

- Ghorbani, H. R.; *Orient. J. Chem.*, **2014**, *30*.
- Yusuff, A. S.; Popoola, L. T.; Aderibigbe, E. I. *J. Environ. Chem. Eng.*, **2020**, *8*, 103907.
- Mirzaei, H.; Darroudi, M.; *Ceram. Int.*, **2017**, *43*, 907.
- Xu, H.; Liu, X.; Cui, D.; Li, M.; Jiang, M. *Sens. Actuators B*, **2006**, *114*, 301.
- Wei, A.; Pan, L.; Huang, W., *Mater. Sci. Eng.*, **2011**, *176*, 1409.
- Mishra, P. K.; Mishra, H.; Ekielski, A.; Talegaonkar, S.; Vaidya, B., *Drug Discov. Today*, **2017**, *22*, 1825.
- Yadav, A.; Mondal, K.; Gupta, A.; *Metal Oxides*, **2022**, 407-435.
- Upadhyay, P.K.; Jain, V. K.; Sharma K.; Sharma, R.; *Res. J. Pharm. Technol.*, **2020**, *13*, 1636.
- Xiong, H. M.; *Adv. Mater.*, **2013**, *25*, 5329.
- Zhu, P.; Weng, Z.; Li, X.; Liu, X.; Wu, S.; Yeung, K.W.K.; Wang, X.; Cui, Z.; Yang X.; Chu, K.; *Adv. Mater. Interfaces*, **2016**, *3*, 1500494.
- Sangeetha, J.; Thangadurai, D.; Hospet, R.; Purushotham, P.; Manowade, K.R.; Jogaiah, S.; *Nanotechnology: An agricultural Paradigm*, **2017**, 33.
- Hamid, R. G.; Hosein, A.; Ali, A. S.; Mahdi, R.; *Asian J. Chem.*, **2011**, *23*, 5111-5118.
- Hamid, R. G.; *Chem. Eng. Commun.*, **2015**, *202*, 1463-1467.
- Moorthy, S. K.; Ashok, C. H.; Rao K. V.; Viswanathan, C.; *Mater. Today: Proc.*, **2015**, *2*, 4360.
- Shameli, K.; Ahmad, M. B.; Al-Mulla, E. A. J.; Ibrahim, N. A.; Shabanzadeh, P.; Rustaiyan, A.; Abdollahi, Y.; Bagheri, S.; Abdolmohammadi, S.; Usman M. S.; Zidan, M.; *Molecules*, **2012**, *17*, 8506.
- Rambabua, K.; Bharatha, G.; Banata, F.; S how, P. L.; *J. Hazard. Mater.*, **2021**, *402*, 123560.
- Jayaseelana, C.; Ramkumar, R.; Rahumana, A. A.; Perumal, P.; *Ind. Crops Prod.*, **2013**, *45*, 423.
- Nnadozie, E. C.; Ajibade, P. A.; *Mater. Lett.*, **2020**, *263*, 127145.
- Khodashenas, B.; Ghorbani, H.R.; *IET Nanobiotechnol.*, **2016**, *10*, 158-161.
- Youssef, A.; Abderrazak, L.; Bouchaib, H.; Abderraouf, R.; Philippe, T.; Meryane, S.; *Optic. Quant. Electr.*, **2014**, *46*, 229-234.
- Roxy, M.S.; Ananthu, A.; Sumithranand, V.B.; *Int. J. Sci. Res. Sci. Eng. Technol.*, **2021**, *8*, 134-139.
- Ghorbani, H. R.; Fazeli, I.; Fallahi, A. A.; *Orient. J. Chem.*, **2015**, *31*.
- Kolekar, T.V.; Yadav, H.M.; Bandgar, S.S.; Deshmukh, P.Y.; *Indian Streams Res. J.*, **2011**, *1*.
- Kittel, C.; *Introduction to Solid State Physics*, **2005**
- Smith, R. A.; *Semiconductors*, **1978**.
- Chakma, S.; Bhasarkar, J. B.; Moholkar, V. S.; *Int. J. Res. Eng. Technol.*, **2013**, *2*, 177.
- Nagaraj, E.; Karuppanan, K.; Shanmugam, P.; Venugopal, S.; *J. Cluster Sci.*, **2019**, *30*, 1157.
- Coates, J.; *Encyclopedia of Analytical Chemistry*, **2006**.
- Hamid, R. G.; *IET Nanobiotechnol.*, **2014**, *8*, 263-266.
- Hamid, R. G.; Mazaher, M.; *Mat. Res. Express*, **2017**, *4*, 65017.